13TH CANADIAN MASONRY SYMPOSIUM
HALIFAX, CANADA
JUNE 4TH – JUNE 7TH 2017

NEW DESIGN DETAIL FOR PARTIALLY-GROUTED MASONRY WALLS

Bolhassani, Mohammad[1] and Hamid, A. Ahmad[2]

ABSTRACT

Partially-grouted masonry structures traditionally have been built using single reinforced grouted vertical cells and horizontal bond beams. Special reinforced fully-grouted masonry walls in high seismic design category have shown acceptable performance. However, this is not the case for ordinary reinforced partially-grouted masonry walls with grout spacing exceeding 4 ft (1.2 m) as demonstrated by recent experimental studies. One simple proposed method to solve the low shear strength and limited displacement ductility of such walls is to simply fully grout the cells or limit their use to low seismic areas. Each of these two solutions has its own pros and cons as it was found and discussed in the literature. Alternative option proposed in this study is to reinforce and grout two adjacent vertical cells and two courses of bond beams instead of one using the same amount of steel ratio. Seven full-scale partially-grouted masonry walls were built and tested as part of NSF/NEES project using conventional and proposed reinforcement details. Different parameters such as the effect of axial load, use of joint reinforcement and wall aspect ratio were investigated. Results demonstrated that the proposed new reinforcement detail resulted in a significant improvement of wall shear strength and deformation capacity.

KEYWORDS: *partially-grouted concrete masonry, fully grouted concrete masonry, shear walls, reinforcement details, seismic performance*

INTRODUCTION

Masonry bearing wall buildings remain one of the relatively less studied structural systems particularly for partially grouted (PG) reinforced masonry construction, a common building system in the eastern United States [1-10]. PG walls are sub-branch of reinforced masonry in which only the reinforced cells are grouted while all other cells are hollow (ungrouted). This detail essentially can make the behavior of such walls significantly different. While most of the reinforced masonry construction in the West Coast is fully grouted (FG), almost all reinforced

[1] Research fellow, Department of Civil Architectural and Environmental Engineering, Drexel University, Philadelphia, PA, mb3238@drexel.edu.
[2] Professor, Department of Civil, Architectural and Environmental Engineering, Drexel University, Philadelphia, PA, hamidaa@drexel.edu.

masonry structures constructed outside the West Coast, including those in regions of high seismic risk, are PG. Partially grouted walls using the conventional single reinforced vertical cells and bond beams detail (SR) do not have adequate seismic performance in areas of high seismicity [11-13]. Experimental tests conducted by Schultz [2, 11] and Minaie et al. [12] showed that PG walls are highly vulnerable to shear failure with reduced shear strength and lower displacement ductility compared to similar FG walls. The ungrouted panels between the grouted masonry elements create a weak zone vulnerable to shear failure. The use of double (i.e., side-by-side) reinforced vertical cells and two course of bond beams (DR) with or without or bed joint reinforcement is proposed here to improve shear strength and ductility capacity over walls with single reinforced cells.

EXPERIMENTAL PROGRAM

Seven full-scale PG masonry shear walls were tested; namely, W1 and W5 walls with SR detail under 20 psi (0.14 MPa) [with aspect ratios of 1.0 and 0.67], W2 and W6 walls with DR detail under 20 psi (0.14 MPa) [with aspect ratios of 1.0 and 0.67], W3 and W7 walls with DR detail with joint reinforcement under 20 psi (0.14 MPa) [with aspect ratios of 1.0 and 0.67], and W4 with DR detail under 100 psi (0.7 MPa) axial compression load were tested under constant axial compressive stress and increasing lateral top cyclic displacement. More details can be found in [14, 15]. Different configurations tested in the experimental part of this paper are presented in the Table 1. Additionally, assemblages test were conducted and results were presented in [16-17].

Table 1: Dimensions and reinforcement configurations of test specimens

Wall ID.	H	L	W	H/L	Reinforcement		Axial stress psi (MPa)
	in. (m)				Vertical	Horizontal	
W1	152 (3.9)	152 (3.9)	7.6 (0.2)	1.0	#6 (D19)	#6 (D19)	20 (0.14)
W2					2#4 (D13)	2#4 (D13)	
W3					2#4 (D13)	2#4 (D13)+JR	
W4					2#4 (D13)	2#4 (D13)	100 (0.70)
W5		224 (5.7)		0.67	#6 (D19)	#6 (D19)	20 (0.14)
W6					2#4 (D13)	2#4 (D13)	
W7					2#4 (D13)	2#4 (D13)+JR	

All details of the walls with different aspect ratios were duplicated except for walls W3 and W7. Reinforced double bond beams with JR at every other course were used in wall W3. However, it changed to a single bond beam with joint reinforcement at every course in W7 wall. The reinforcement of the first specimen, W1, had #6 (D 19) bars spaced at 72 in. (1.8 m) on center in the vertical and horizontal directions. However, the reinforcement configuration for the rest of specimens were the same using 2 #4 (D13) bars in each direction except for DS-J-0.67-20 wall with 1 #4 (D13) for bound beams and 2#4 (D13) for vertical grouted cells. Figure 1 shows the detail of all specimens. Note that wall W4 construction details were the same as for wall W2. Therefore, the details were not repeated. Vertical reinforcement in W1 and DS-1.0-20 specimens

consisted of 1#6 (D19) and 2#4 (D13), respectively as shown in Figure 1-b and 1-d. Wall W3 has the same vertical and horizontal steel as wall W2 with the addition of ladder-type joint reinforcement every other course as shown in Figure 1-f. All specimens have a vertical reinforcement ratio of approximately 0.1% of the net cross section area.

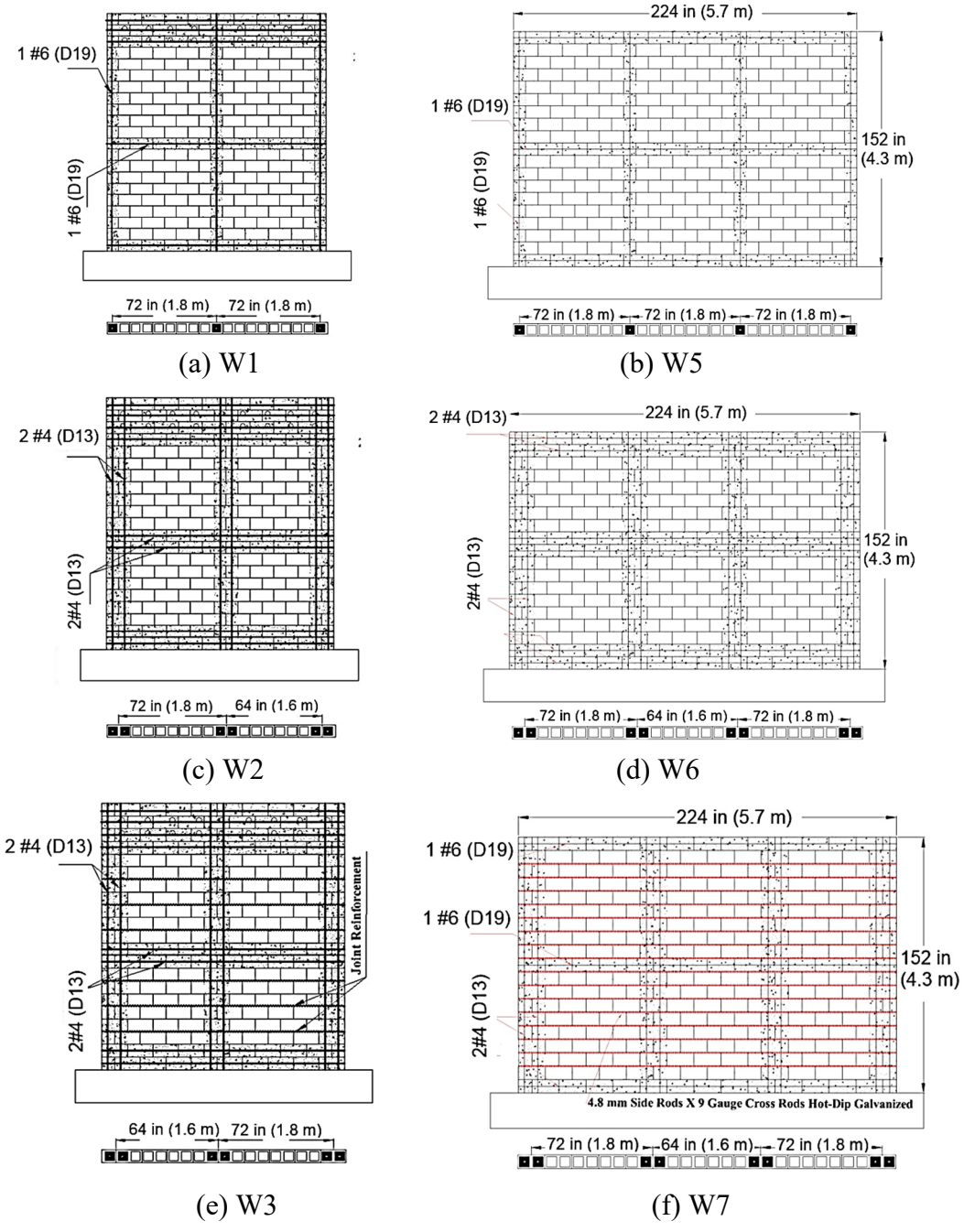

Figure 1: Wall specimens and reinforcement configurations

However, horizontal reinforcement ratios of W1, W2 and W7 walls were equal to 0.08%, 0.08% and 0.1%, respectively. Wall W7 has the same vertical steel as for wall W6. However, the horizontal steel consisted of one steel bar in bond beams with the addition of ladder-type joint reinforcement every course as shown in Figure 1-e. W5, W6 and W7 specimens have vertical steel ratio of approximately 0.103%, 0.094% and 0.094% of the net area, respectively. Horizontal steel ratio of W5, W6 and W7 walls were equal to 0.072%, 0.073%, and 0.069%, respectively. This difference in the horizontal steel ratio is due to presence of joint reinforcement in wall W7 instead of steel bars in bond beams. Net area of walls was calculated based on the hollow section by considering the mortar face shells, the webs and the area of grouted cells. It worth mentioning that these walls are considered the largest PG masonry shear walls ever tested and reported in the literature.

EXPERIMENTAL RESULTS

Crack pattern and failure mode

All specimens approximately displayed the same elastic behavior up to 0.05% drift and a load of about 25 kips (113 kN). No visible cracks occurred at this low drift level. A few flexural bed and head joint cracks appeared at 0.2% drift, in all specimens. Additionally, diagonal zigzag de-bonding joint cracks developed in the hollow (ungrouted) portions of the walls and diagonal cracks were observed at the bottom and top parts simultaneously at roughly 0.3% drift for all specimens. Diagonal cracks propagated in a step pattern due to weak mortar bond along the bed and head joints. The number of cracks initiated in the ungrouted masonry and then propagated into the grouted cells in W1 and W5 walls are significantly more than W2, W6 and W7 walls. In general, cracks in the specimen designed based on TMS 402 cod's provisions [18], (W1 and W5 walls), were wider than the specimens with proposed reinforcing detail. Test observation also showed that distribution of vertical cracks in the vertically grouted cells was only limited to W1 and W5 walls. Toe crushing did not occurred in walls W6 and W7. Step cracks constituted the majority of walls W1 and W5 cracks. However, a combination of flexural cracks, horizontal cracks, and step cracks existed in walls W2 and W6. Both W6 and W7 walls exhibited a shear dominated failure. Although many horizontal cracks were observed between joints, no signs of bar yielding observed at the toe regions and both walls were failed in shear mode. However, due to enhanced configuration, higher deformation capacity was achieved before failure. The distribution of cracks in wall W3 and W7 were significantly higher than for walls W2 and W6, particularly at the top. This demonstrated that joint reinforcement was effective and instead of forming step cracks flexural cracks took in place. Cracks were distributed uniformly in order of size and amount in W3 and W7 specimens.

Load-displacement hysteretic curves

Figure 2 shows the top lateral force-lateral displacement of all specimens. Sliding displacements at the bottom of specimens were subtracted from these curves. W1, W4 and W5 walls exhibited a brittle shear mode failure as evident from the drastic post-peak strength degradation of the

hysteresis loops while W6 and W7 showed a more stable post-peak response and a higher deformation capacity. Additionally, W2 and W3 walls exhibited a ductile shear failure mode. The rapid post-peak strength degradation of the W1 and W5 walls is the major drawback of conventional design detail that was overcame by using the proposed double reinforcing cells/bond beams in W2 and W3 walls. Wall W1 with single reinforcement detail (SR) displayed a rocking behavior causing toe crushing whereas for wall W2 with double reinforcing detail (DR), more horizontal cracks and sliding between the bottom courses were developed resulting in a more ductile behavior with large strength and deformation capacity (see Figure 3).

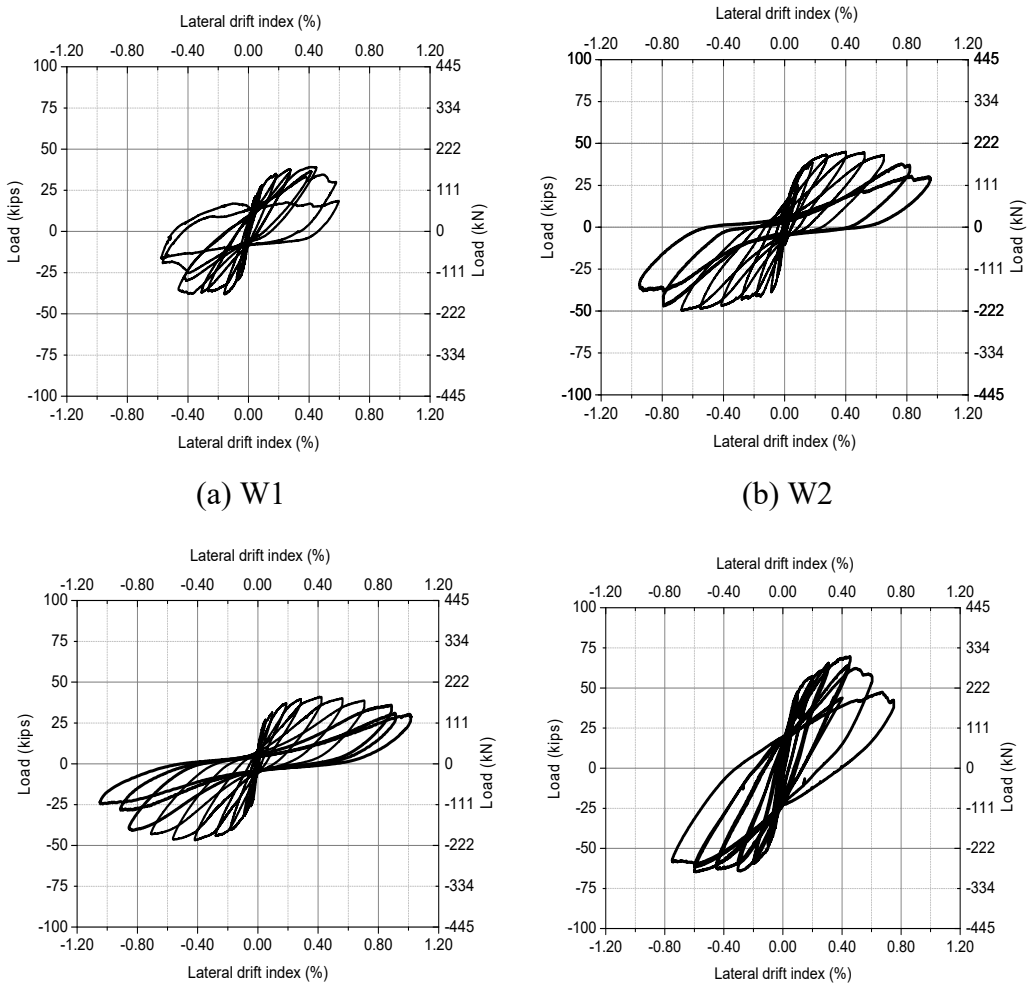

(a) W1 (b) W2

(c) W3 (d) W4

Figure 2: Lateral force displacement hysteresis loops

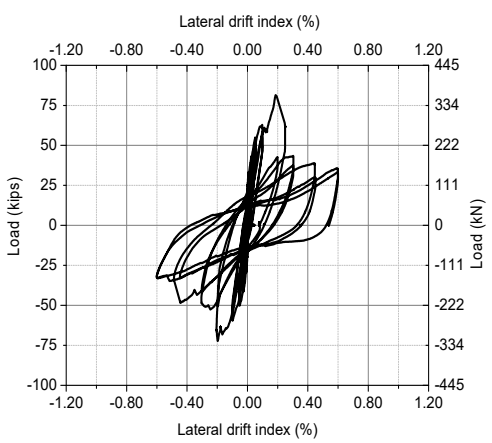

(e) W5

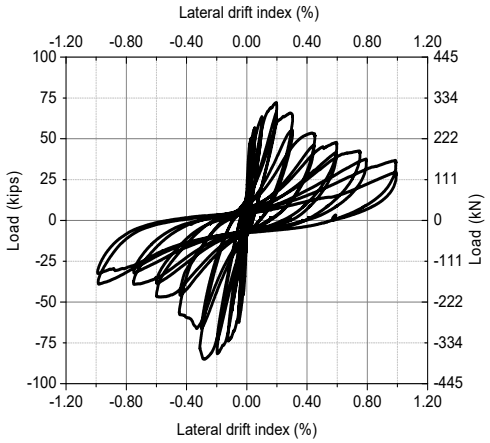

(f) W6

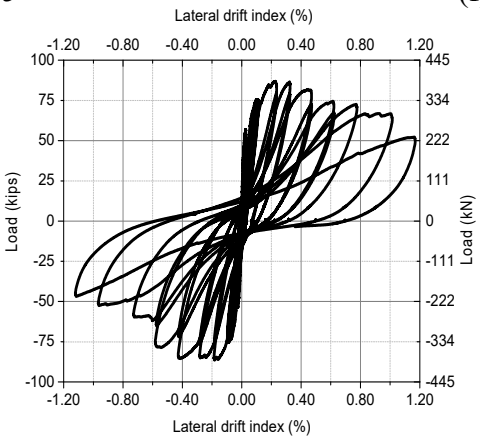

(g) W7

Figure 2: Lateral force displacement hysteresis loops (continued)

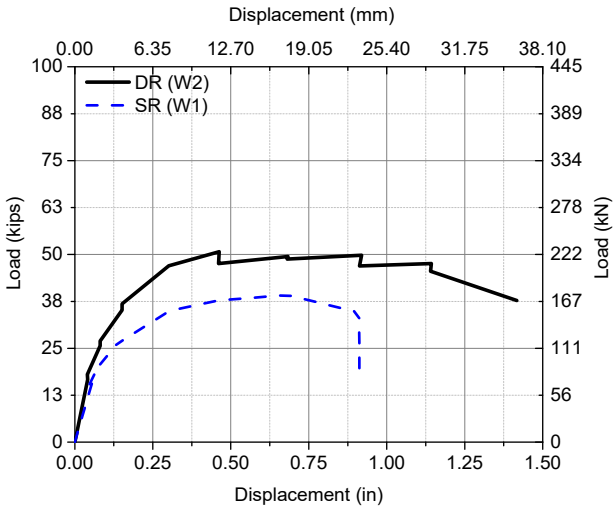

Figure 3: Effect of reinforcing detail on wall response

As shown in Figure 4, the increase of axial stress resulted in a higher strength and a lower deformation capacity. Less bed joints sliding, because of higher frictional resistance due to higher axial stress, was apparent in wall W4 compared to wall W2.

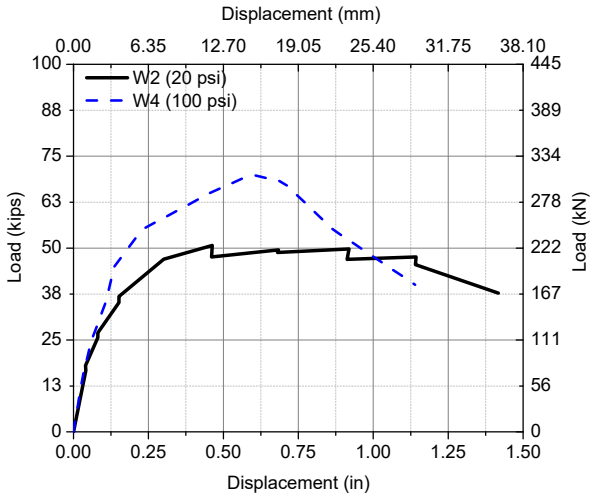

Figure 4: Effect of axial load on wall response

Test results showed that the aspect ratio has a significant impact on wall behavior. Reducing the aspect ratio of single reinforced grouted cells/bond beams wall from 1.0 to 0.67 resulted in an increase the shear strength by 380%. However, as expected, maximum displacement of the wall decreased significantly (see Figure 5-a). The same behavior was observed in doubly reinforced grouted cells/bond beams wall (Figure 5-b). Shear capacity increased significantly (by 251%), however, maximum displacement decreased.

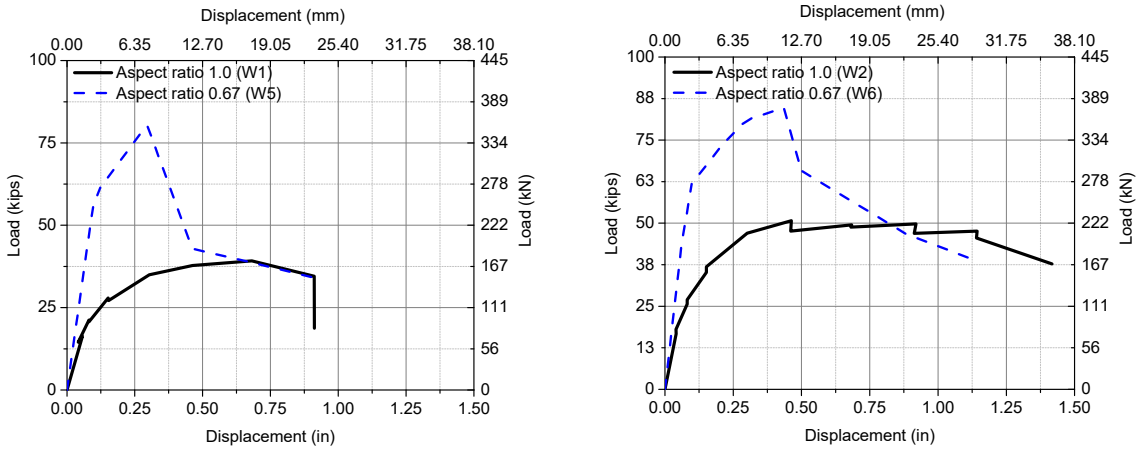

(a) SR walls (b) DR walls

Figure 5: Effect of the aspect ratio on wall response

For walls with aspect ratio of 0.67 test results demonstrate that SR wall (W5) had nearly the same shear capacity as DR walls (W6, W7). However, wall deformability increased significantly. As can be seen from Figure 6, the addition of joint reinforcement to DR walls resulted in a more stable post-peak response and larger deformation capacity.

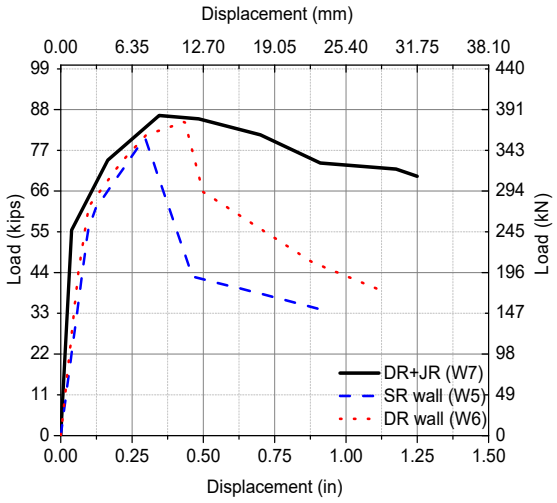

Figure 6: Effect of reinforcement configuration on wall response

Wall shear strength

Table 2 presents a summary of recorded experimental results of the tested walls such as shear strength, stiffness and failure mode. Predicted shear strength of all specimens (V_n) using the following TMS 402 shear expression [18] were also calculated and shown in Table 2.

$$V_n = \left\{ \left[4 - 1.75 \left(\frac{M_u}{V_u d_v} \right) \right] A_n \sqrt{f'_m} + 0.25 P_u + 0.5 \left(\frac{A_v}{s} \right) f_y d_v \right\} \cdot \gamma_g \quad (1)$$

Where, γ_g is a reduction factor, equal to 0.75, to account for the effect of partial grouting in reducing the shear strength as demonstrated in past research, A_n is net cross-sectional area, f'_m is compressive strength of masonry prism and P_u is level of axial load. Shear reinforcement term in the code's expression is calculated on the basis of $0.5A_h f_{yh} d_v/s_h$. This term is associated with the horizontal reinforcement area and the spacing of horizontal grouted bond beams. As shown in Table 2, the code equation over-estimates the shear strength of W1, W2, W3, W4, W5, W6 and W7 walls by 88, 65, 65, 32, 78, 85 and 61 percent, respectively.

Table 2: Wall test results

Wall ID.	Peak load kips (kN)		V_u Shear strength kips (kN)	V_n (TMS 402) kips (kN)	Stiffness kip/ft (kN/m)
	Positive	Negative			
W1	39 (175)	37 (165)	39 (175)	71 (316)	5 (72.5)
W2	45 (200)	51 (227)	51 (227)	82 (365)	7.4 (108)
W3	45 (200)	47 (208)	47 (208)	82 (365)	7.4 (108)
W4	70 (309)	66 (295)	70 (309)	92 (409)	10 (150)
W5	80 (358)	74 (330)	80 (358)	144 (639)	24 (358)
W6	71 (316)	85 (380)	85 (380)	157 (696)	26 (377)
W7	87 (387)	85 (378)	87 (387)	139 (619)	27 (384)

The proposed double horizontal reinforcing cells delayed the propagation of diagonal shear cracks and enabled the distribution of stresses over the entire wall after the onsets of major diagonal cracks. Therefore, wall W2 with DR detail showed gradual post-peak strength degradation. This significant increase in wall capacity could be attributed to the ability of the connection between the grouted reinforced cells and the reinforced bond beam, in case of DR walls, to carry moment (Figure 7). However, as showed in the idealized model, the connections in the SR wall acting as a pin that cannot carry moment.

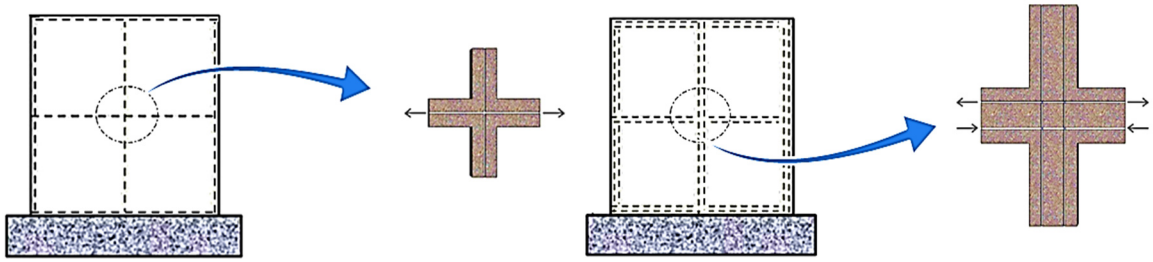

Figure 7: Connection of vertical grouted cells and horizontal bond beams

These moment-carrying connections resulted in more ductile response, by increasing the number of plastic hinges in the structure. This explanation assumes an infilled frame behavior at the ultimate limit state. In wall W1, before forming cracks at the edges, stepped diagonal shear cracks in the center of the hollow panels initialized. The size of cracks at the middle of the hollow panels increased as the lateral displacement increased. By increasing the lateral load, cracks initiated at the edge of the hollow panels close to the grouted cells. However, these cracks propagated in the grouted cells because weak connection in SR walls between the lower beam and the vertical grouted cells. Therefore, the coupling effect cannot be developed and a large portion of the load was transferred directly through the struts to the wall toes resulting in toe crushing at the edges.

CONCLUSIONS

Based on the test results reported herein, the following conclusions are drawn:

1-The experimental results indicated that the proposed doubly grouted reinforcement detail significantly improved seismic performance of partially grouted reinforced masonry shear walls compared with the conventional singly grouted detail. Specifically, W2 (with DR detail) wall exhibited a 34% increase in shear capacity and 47% increase in displacement ductility compared to W1 wall with SR detail.

2- Wall W3 exhibited nearly identical performance as W2 wall indicating that the addition of joint reinforcement at every other course for DR walls has a minimal influence on improving wall seismic performance. Wall W2 showed a higher deformation capacity compared to W4 wall. It is, therefore, concluded that increasing the axial load from 20 psi (0.14 MPa) to 100 (0.7 MPa) psi resulted in an increase the shear capacity by 40 percent and a decrease in displacement ductility by 50 percent.

3- Changing the aspect ratio of the wall from 1.0 to 0.67 resulted in an increase in shear capacity of W1 and W2 walls by order of 113 and 70%, respectively. Although the detail of W3 was different from W7, changing the aspect ratio increased the shear capacity of the wall by 85%. Test results also demonstrated that W5 wall had a brittle shear-dominated mode and using DR detail and joint reinforcement (W7) changed the brittle shear failure mode to a ductile shear mode.

4- Although, the proposed W6 and W7 details had a marginal effect on increasing the wall shear strength compared to W5, they dramatically increased the ductility of specimens by 50% and 405%, respectively.

REFERENCES

[1] Nolph, S. and ElGawady, M. (2012). "Static cyclic response of partially grouted masonry shear walls." *Journal of Structural Engineering*, 138(7):864-879.

[2] Schultz, AE. (1996). "Seismic resistance of partially grouted masonry shear walls*." In: The Worldwide Advances in Structural Concrete and Masonry*.

[3] Voon, K. C. and Ingham, J. M. (2006). "Experimental in-plane shear strength investigation of reinforced concrete masonry walls." *Journal of Structural Engineering*,132(3):400-408.

[4] Ghanem, G. M. (1992). "Effect of steel distribution on the behavior of partially reinforced masonry shear walls." *In: proceeding of 6th Canadian Masonry Symposium*, Univ. of Saskatchewan, Saskatoon, Sask., Canada, pp. 356-376.

[5] Maleki, M. (2008). "*Behavior of partially grouted reinforced masonry shear walls under cyclic reversed loads*." Ph.D. thesis, McMaster Univ., Hamilton, Ont., Canada.

[6] Bolhassani, M., Hamid, A. A., Rajaram, S., Vanniamparambil, P. A., Bartoli, I., Kontsos, A. (2017). "Failure analysis and damage detection of partially grouted masonry walls by enhancing deformation measurement using DIC." *Engineering Structures Journal*, 134: 262-275.

[7] Khan, F., Rajaram, S., Vanniamparambil, P. A., Bolhassani, M., Hamid, A. A., Kontsos, A., Bartoli, I. (2015). "Multi-sensing NDT for damage assessment of concrete masonry walls." *Structural Control and Health Monitoring*, no. 3,22: 449-462.

[8] Khan, F., Bolhassani, M., Kontsos, A., Hamid, A. A., Bartoli, I. (2015). "Modeling and experimental implementation of infrared thermography on concrete masonry structures." *Infrared Physics & Technology*, 69: 228-237.

[9] Ghanem, G. M., Salama, A. E., Elmagd, S. A., Hamid, A. A. (1993). "Effect of axial compression on the behavior of partially reinforced masonry shear walls." *Proc., 6th North American Masonry Conf. (NAMC)*, Philadelphia, 1145-1157.

[10] Voon, K. C, Ingham, J. M. (2006). "Experimental in-plane shear strength investigation of reinforced concrete masonry walls." *Journal of Structural Engineering*, 132(3):400-408.

[11] Schultz, A. E., and Hutchinson, R. S. (2001). "Seismic Behavior of Partially-Grouted Masonry Shear Walls, Phase 2: Effectiveness of Bed-Joint Reinforcement." GCR 01-808, National Institute of Standards and Technology, Gaithersburg, MD, 442 pp.

[12] Minaie, E., Mota, M., Moon, F. L., Hamid, A. A. (2010). "In-plane behavior of partially grouted reinforced concrete masonry shear walls." *Journal of Structural Engineering*, 136(9):1089-1097.

[13] Nolph, S. M. (2010). "In–plane shear performance of partially grouted masonry shear walls." Master's thesis, Washington State University, Pullman, WA.

[14] Bolhassani, M. Hamid, A. A., Moon, F. L. (2015). "Enhancement of In-Plane Capacity of Partially Grouted Concrete Masonry Shear Walls." *Engineering Structures Journal*, 108: 59-76.

[15] Bolhassani, M., Hamid, A. A., Johnson, C., Moon, F. L., Schultz, A. E. (2016). "New design detail to enhance the seismic performance of ordinary reinforced partially grouted masonry structures." *Journal of Structural Engineering*, 142(12):04016142.

[16] Hamid, A. A., Bolhassani, M., Turner, A., Minaei, E., Moon, F. L. (2013). "Mechanical properties of ungrouted and grouted concrete masonry assemblages." *12th Canadian Masonry Symposium*, Vancouver, British Columbia.

[17] Bolhassani, M., Hamid, A. A., Lau, A. C., Moon, F. (2015). "Simplified micro modeling of partially grouted masonry assemblages." *Construction and Building Materials*, 83:159-173.

[18] Building code requirements for masonry structures. (2013). TMS 402, ACI 530, and ASCE 5, The Masonry Institute, Boulder, American Concrete Institute, ASCE, Farmington Hills, MI, Reston, VA.